





Stability Constraints on Reliability-Oriented Control of AC Microgrids – Theoretical Margin and Solutions

Yubo Song , *Student Member, IEEE*, Subham Sahoo , *Senior Member, IEEE*,
Yongheng Yang , *Senior Member, IEEE*, and Frede Blaabjerg , *Fellow, IEEE*

Abstract—Reliability is of importance for operation maintenance and cost reduction in power electronics and systems. Based on the reliability models of power devices, reliability-oriented power sharing in microgrids enforces the redistribution of power among converters to prolong the lifetime of the entire system, and droop control is typically used herein. However, this could affect the system stability, which contradicts the prerequisite of secure operation. In light of the above, this article is aimed to reveal this limitation of reliability-oriented droop control and emphasize its impact on system stability. Accordingly, a framework of stability-constrained reliability-oriented droop control is proposed, together with solutions that can help to enhance the stability. With this, the reliability of the system could be further improved without violating the stability criteria. Moreover, experimental tests and long-term reliability evaluations are included, which demonstrates that the aforementioned issues can be effectively addressed alongside with the proposed framework and solutions.

Index Terms—AC microgrids, droop control, power distribution, power electronic systems, reliability, stability.

I. INTRODUCTION

THE development of power electronics is benefiting industrial applications and the utilization of renewable energy sources (RESs) [1], [2]. In practice, electrical or thermal stresses are seen as the main causes of degradation and possible failures of the devices in systems. As a result, the functionality of the entire system may be influenced, and additional economic costs are required for maintenance [3]. The issue becomes significant, especially when the RES with various mission profiles are highly penetrating into the system. This may contribute much to extra stresses on components [3].

Reliability of power electronics and systems is consequently attracting much attention. Reliability indicates the ability that a

component or system is functioning well as per the requirements [4], which are normally used to plan the maintenance and achieve lower economic costs [5]. The reliability of devices or systems can be measured by the probability of failures (unreliability), or the estimated length of time before a failure appears (lifetime). There are mathematical approaches in reliability engineering like [6] and [7], but in the field of power electronics, much emphasis has been put on the failure mechanisms, so that the reliability can be improved in a more targeted way [8].

Based on this, the reliability of power electronic systems is thereby derived considering the functional relationship of the components inside it [9], [10], wherein reliability-oriented design and power sharing are proposed to prolong the lifetime of the entire system considering all components. In power electronic converters, the stresses on the components are redistributed [11], while in multi-converter systems like microgrids, secondary or in certain cases tertiary controllers are normally used to plan the power sharing among the converters [12], [13], [14]. The basic rule is that more fragile parts or the parts with shorter lifetime should undertake less stresses.

However, system stability is often not considered for analysis as reliability analysis is normally performed in long timescale with probabilistic approaches. Stability is the ability of a system to reach a steady state after a disturbance [15], and reflects if the system can operate securely, e.g., without abnormal oscillations or power outage. There are mainly two stability modeling approaches: state-space-based [16] and impedance-based approaches [17], [18], which have been compared and quantitatively mapped in [19]. A system can become unstable when there is, e.g., a mismatch in system parameters, a sudden fault, or a power disturbance beyond the adjustability of the system [15], [20].

In the literature, the studied systems are always assumed to be stable throughout its entire lifetime. For example, the frequency and voltage limits are not considered when designing the power flow in [21], and the control parameters in the reliability-oriented power sharing in [13] are adjusted only considering the accumulated damage in the devices. Though stability corresponds to a smaller timescale, it is a necessity for systems to function well in the long term, and instability issues are not negligible herein, which is not addressed in the literature. It is thereby of significance to integrate the stability analysis into reliability evaluations in order to formalize the reliability-oriented design with more stability constraints for both reliable and secure power supply.

Manuscript received 24 November 2022; revised 15 February 2023; accepted 22 April 2023. Date of publication 26 April 2023; date of current version 21 June 2023. This work is supported mainly by the Reliable Power Electronic-Based Power System (REPEPS) project at Department of Energy, Aalborg University, as a part of the Villum Investigator Program funded by the Villum Foundation, Denmark, in part by the National Natural Science Foundation of China through the Project 52107212, and in part by the Zhejiang Kunpeng Investigator Program. Recommended for publication by Associate Editor M. Molinas. (*Corresponding authors: Yubo Song; Yongheng Yang.*)

Yubo Song, Subham Sahoo, and Frede Blaabjerg are with the Department of Energy, Aalborg University (AAU Energy), 9220 Aalborg East, Denmark (e-mail: yuboso@energy.aau.dk; sssa@energy.aau.dk; fbl@energy.aau.dk).

Yongheng Yang is with the College of Electrical Engineering, Zhejiang University, Hangzhou 310027, China (e-mail: yoy@zju.edu.cn).

Color versions of one or more figures in this article are available at <https://doi.org/10.1109/TPEL.2023.3270640>.

Digital Object Identifier 10.1109/TPEL.2023.3270640

Therefore, this article is aimed to look into this issue and emphasize the role of stability in the reliable operation of microgrids, and proposes a framework of stability-constrained reliability-oriented droop control for microgrid systems. Stability analysis is performed under the scenario of reliability-oriented control. Potential instability is revealed accordingly, and the system reliability should be bounded by stability criteria, which is an intuitive connection between the two indices. Certain solutions for stabilizing the system are presented, with which the system reliability can be further improved.

The rest of this article is organized as following. Section II presents reliability-oriented power sharing in microgrids, and the stability of a multiconverter microgrid with reliability-oriented droop control is modeled in Section III, together with practical solutions to stability enhancement. A framework of stability-constrained reliability-oriented droop control is proposed and explained in Section IV. Moreover, experiments and long-term reliability analysis are presented in Section V, illustrating the significance of stability analysis and the effectiveness of the stabilizing techniques for reliability-oriented droop control. Finally, Section VI concludes this article.

II. RELIABILITY-ORIENTED POWER SHARING IN MICROGRIDS

A. Reliability of Power Converters and Microgrids

To evaluate the system-level reliability of a microgrid, it is first decomposed into smaller parts, such as converters, loads, lines and filters. In this article, the influence of power converters is focused on, which is dependent on the electrothermal stress and the reliability of power components. It is investigated in [22] that power semiconductors and capacitors are among the most fragile components in power converters. Thus, their lifetime models are introduced in this section considering mission profiles in power electronic applications.

One of the most commonly-used lifetime model of power semiconductors is given in (1) [23], where the lifetime is mainly determined by the average junction temperature T_{jm} and the swing of the junction temperature ΔT_j

$$N_f = A \cdot \Delta T_j^\alpha \cdot \exp\left(\frac{\beta_1}{T_{jm}}\right) \cdot t_{on}^\gamma \quad (1)$$

in which, A , α , β_1 , and γ are the constant coefficients obtained through power-cycling tests [24].

Based on the Miner's rule [25], the accumulated damage of power semiconductors is the sum of damage in all time intervals from the initial state, as

$$D_{sw} = \sum_i \frac{n^{(i)}}{N_f^{(i)}} \quad (2)$$

where $n^{(i)}$ and $N_f^{(i)}$ are the counted number of power cycles in the i th time interval and the rated cycles-to-failure under the corresponding mission profile, respectively. By the end of life (EOL) for a device, the accumulated damage should be 1.

The lifetime of capacitors is calculated from the voltage and its corresponding loading condition [26], as

$$L = L_0 \cdot 2^{\frac{T_0 - T}{n_1}} \cdot \left(\frac{V}{V_0}\right)^{-n_2} \quad (3)$$

where V and T are the voltage and temperature at use, V_0 and T_0 are those in rated conditions, L_0 is the rated lifetime, and n_1 and n_2 are constant coefficients.

The accumulated damage of capacitors is expressed as

$$D_{cap} = \sum_i \frac{\Delta t^{(i)}}{L^{(i)}} \quad (4)$$

with $\Delta t^{(i)}$ and $L^{(i)}$ being the duration of the i th time interval and rated lifetime under corresponding mission profile, respectively. By the EOL, the accumulated damage should also be 1.

The time-to-failure data of components over time follows Weibull distribution. Therefore, the reliability of a device in a system can be described by the cumulative density function as

$$R(t) = \exp\left[-\left(\frac{t}{\eta}\right)^\beta\right] \quad (5)$$

where β is the shaping parameter in the Weibull distribution, and η is the characteristic lifetime of the component. The estimated lifetime obtained from (2) and (4) is normally referred to as the B_{10} lifetime in (5), namely the time t when the reliability of the component $R(t)$ decreases to 90%, or 10% of the device population fail to operate.

Assuming that there are no parallel paths in the reliability block diagram [9], the reliability of a converter R_{conv} is then the multiplication of the reliability of all the components inside. If the total number of fragile components is N , this can be expressed as

$$R_{conv} = \prod_{j=1}^N R^{(j)}. \quad (6)$$

The overall damage or consumed lifetime of a converter with M components can be formulated as the average of the damages of all the considered components [27], as

$$D_{conv} = \frac{1}{M} \sum_{j=1}^M D_{sw \text{ or cap}}^{(j)} \quad (7)$$

where D_{conv} represents the normalized damage of the converter.

If all converters are supposed to operate as per the functional requirements, the system-level reliability R_{MG} should be the multiplication of the reliability of all converters in the system

$$R_{MG} = \prod_{j=1}^M R_{conv}^{(j)}. \quad (8)$$

The entire procedure is thereby illustrated in Fig. 1. The reliability of components is first evaluated based on the mission profiles (loading, ambient temperature or other factors that influence the stresses) and the subsequent thermal and electrical stresses, and the system-level reliability can be derived according to (6)

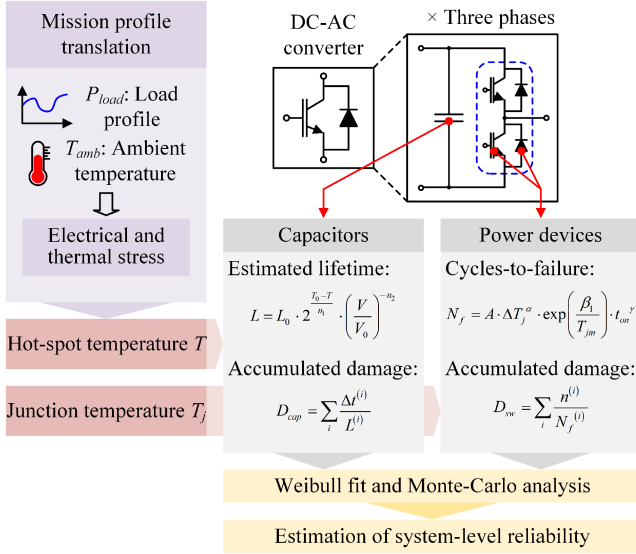


Fig. 1. Evaluation procedure of system-level reliability for a three-phase DC-AC converter.

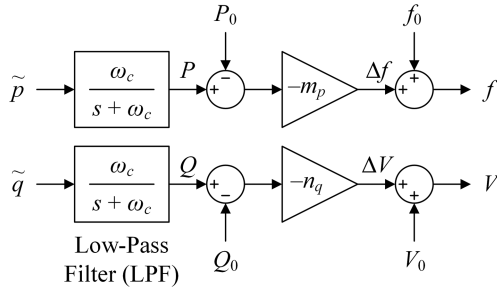


Fig. 2. Droop control in multi-converter microgrid systems, where \tilde{p} and \tilde{q} are the active and reactive power directly calculated from the measured voltage v_o and current i_o .

and (8). Moreover, the Monte Carlo method can be employed when the uncertainty of parameters is considered.

In this article, in order to simplify the analysis, the dc voltage of converters are assumed to be constant without dynamics, and only the degradation of power semiconductors is considered when evaluating the system reliability. There will be similar conclusions if capacitors are also considered.

B. Reliability-Oriented Power Sharing of Microgrids

The overall reliability of a microgrid is dependent on the converter with the lowest reliability. To enhance the overall reliability, the converter consuming more lifetime should share less loading. Thus, the power flow among converters can be adjusted accordingly.

In microgrids, one of the most commonly-used power control strategies is droop control, where the frequency and amplitude of voltage are controlled according to their respective droop relationships with the filtered instantaneous active power P and reactive power Q . It is expressed as (9) and Fig. 2 [28]

$$\begin{aligned} f &= f_0 - m_p (P - P_0) \\ V &= V_0 - n_q (Q - Q_0) \end{aligned} \quad (9)$$

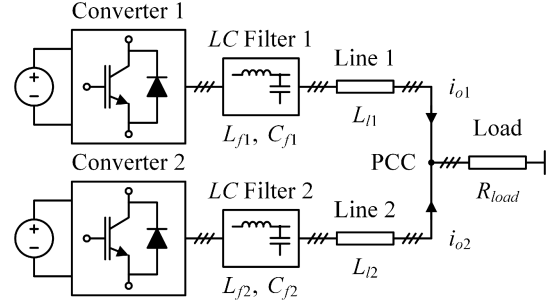


Fig. 3. Topology of the studied three-phase AC microgrid. For each converter, L_f and C_f are the inductance and capacitance of the LC filter, L_l is the inductance of the line, and $i_{o1, 2}$ are the corresponding current flowing into the PCC.

TABLE I
KEY PARAMETERS OF THE STUDIED TWO-CONVERTER SYSTEM

Parameters	Values
Nominal AC voltage V_n	110 V _{RMS} , 50 Hz
Switching frequency f_{sw}	10 kHz
LC Filter inductance L_{f1}, L_{f2}	$L_{f1} = L_{f2} = 2.0$ mH
LC Filter capacitance C_{f1}, C_{f2}	$C_{f1} = C_{f2} = 10$ μ F
Line inductance L_{l1}, L_{l2}	$L_{l1} = L_{l2} = 0.5$ mH
Load resistance R_{load}	3 Ω (12 kW)
Base value of the P - f droop coefficient m_{p0}	9.4×10^{-5} [Hz/W]
Base value of the Q - V droop coefficient n_{q0}	1.3×10^{-3} [V/Var]

Note: V_{RMS} = Volts in Root-Mean-Square (RMS) value.

where (P_0, f_0, Q_0, V_0) is the given nominal operation point, and m_p and n_q are the active and reactive droop gains, respectively.

Subsequently, a reliability-oriented droop control strategy has been introduced in [13] and [29], where the active droop gain m_p is adjusted as

$$m_p = m_{p0} \cdot [\alpha + (1 - \alpha) \cdot \beta_m^\lambda] \quad (10)$$

where β_m is the adjustment coefficient with respect to the accumulated damage D , $0 \leq \alpha \leq 1$ is a weighting factor of the conventional and reliability-oriented droop control, and $\lambda > 0$ indicates the role of D_i in affecting the droop gain m_p .

The adjustment coefficient β_m can be given as [29]

$$\beta_m = \begin{cases} D_0/D_i & \text{if } P < P_0 \\ D_i/D_0 & \text{if } P \geq P_0 \end{cases} \quad (11)$$

where D_0 is the reference value of the accumulated damage. It can be, e.g., either the minimum, maximum or average of the accumulated damage of all converters in the system. In this article, all relevant discussions are based on (10) and (11) unless specifically stated otherwise.

III. STABILITY ANALYSIS OF RELIABILITY-ORIENTED DROOP CONTROL

To illustrate the stability issue with reliability-oriented droop control, a three-phase microgrid consisting of two converters is chosen as an example, which is shown in Fig. 3. Two dc-ac converters operate in parallel at the point of common coupling (PCC). A resistive load is connected to the PCC. The key parameters are given in Table I.

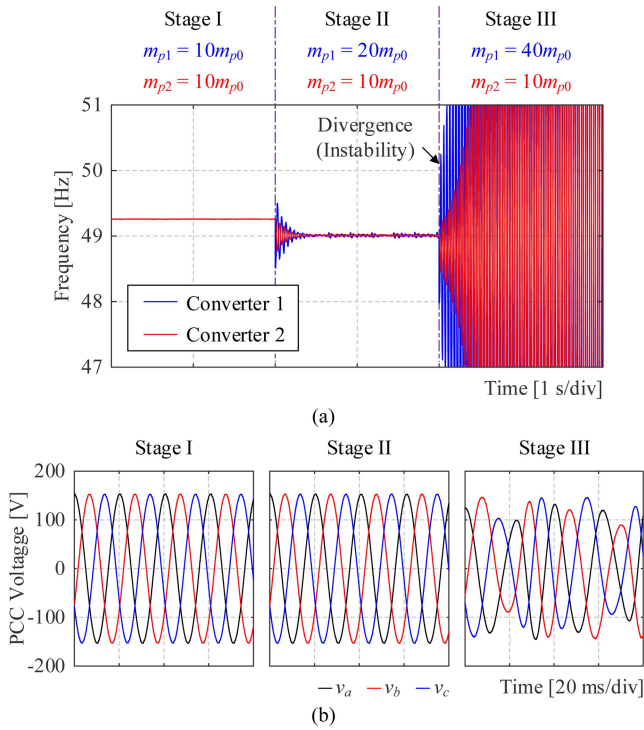


Fig. 4. System performances when the droop gain of converter 1 is increased, including (a) frequency of the two converters, and (b) voltage at the PCC.

A. Stability Modeling of Reliability-Oriented Droop Control

In the reliability-oriented power sharing method in Section II-B, the target is to reduce the loading on the converters consuming more lifetime, which is implemented by adjusting the droop gain. According to (9), given that the frequency f of all converters is equal, the loading on converters increases in accordance with the droop gain m_p when $P < P_0$, and decreases contrarily, when $P > P_0$. It also means that the droop gain should be increased in one or more converters under this scenario. However, this will lead to a stability issue. For example, in Fig. 4, when the droop gain of converter 1 is increased from $10 m_{p0}$ to $20 m_{p0}$, the operation point will move according to (9) with a lower frequency. However, when the droop gain is further increased to $40 m_{p0}$, the frequency becomes divergent, and the instability appears with increasing oscillations. The system cannot continue operating even if all components and converters have not yet worn out.

Nevertheless, the instability can be explained by stability modeling approaches. The state-space-based modeling in [16] is employed in this section. To simplify the analysis, the dynamics of the double voltage loop are neglected unless specified otherwise, and the system is then modeled with the following small-signal state vector $\Delta x_{\text{conv}}^{(k)}$ ($k = 1$ or 2)

$$\Delta x_{\text{conv}}^{(k)} = \Delta \left[\delta^{(k)} \quad P^{(k)} \quad Q^{(k)} \quad i_s^{(k)} \quad v_o^{(k)} \quad i_o^{(k)} \right]^T \quad (12)$$

where i_s and i_o are, respectively, the currents through the filter inductor L_f and the line L_l , and v_o is the output voltage of the converter. The voltage at PCC (load voltage) is then determined

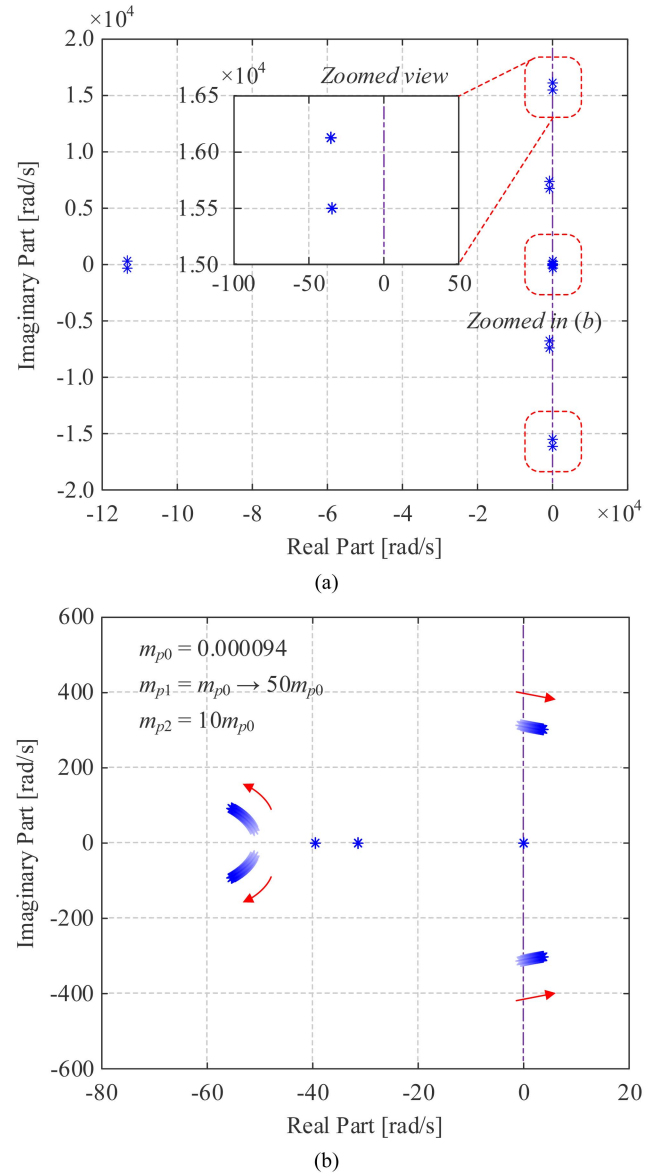


Fig. 5. Eigenvalue loci of the example system when the active droop gain of converter 1 ranges from m_{p0} to $50 m_{p0}$, (a) location of all eigenvalues, and (b) zoomed view of low-frequency modes. A pair of eigenvalues move toward the RHP, indicating the instability.

by the load resistance and the sum of i_{o1} and i_{o2} according to the Kirchhoff's law.

Subsequently, the state space of the microgrid can be constructed as:

$$\frac{d}{dt} \begin{bmatrix} \Delta x_{\text{conv1}} \\ \Delta x_{\text{conv2}} \end{bmatrix} = \mathbf{A}_{\text{MG}} \begin{bmatrix} \Delta x_{\text{conv1}} \\ \Delta x_{\text{conv2}} \end{bmatrix} \quad (13)$$

where \mathbf{A}_{MG} is the state matrix.

With the above model, the eigenvalue loci are plotted in Fig. 5. When the droop gain of Converter 1 is increased from m_{p0} to $50 m_{p0}$, a pair of poles move toward the right-half plane (RHP), which confirms the instability. This instability mode shows an angular frequency (around 300 rad/s) close to the fundamental

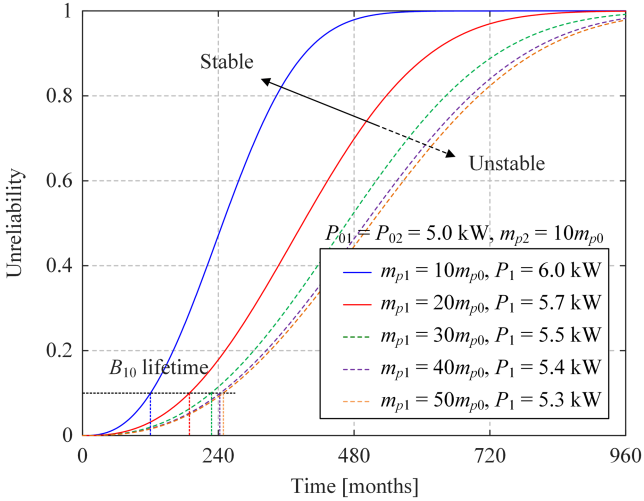


Fig. 6. System unreliability over time when the droop gain of converter 1 changes. The system goes unstable when m_{p1} is larger than $30 m_{p0}$.

frequency ω_1 (314 rad/s), so the instability should be a low-frequency oscillation, which accords with the simulation results.

Based on [15], the instability due to parameter mismatch should be classified as converter instability. Thus, to solve this issue, the modification of controllers is a major focus in the following sections.

B. System-Level Reliability Bounded by Stability Criteria

In addition, the results in Section III-A also mean that the reliability of the entire system is bounded by the stability criteria. To illustrate this concern, reliability evaluation is performed in the study case. The nominal power of both converters is set as 5 kW, and the droop gain as $m_{p2} = 10 m_{p0}$. The power semiconductors in converters 1 and 2 are selected differently as Infineon FS25R12KT3 (1200 V/25 A) and FP30R12KE3 (1200 V/30 A), respectively. To improve the system reliability, Converter 2 with higher power rating is consuming its lifetime more moderately, and should share more loading. Thus, the droop gain of converter 1 is increased.

The system reliability is then evaluated in Fig. 6. As the system is a relatively simple example consisting of only two converters, the B_{10} lifetime of the system ranges around tens of years. For a certain m_{p1} , the power sharing between the two converters can be determined based on the droop relationship (9) and the loading. However, when m_{p1} increases from $10 m_{p0}$ to $50 m_{p0}$, the system goes beyond the stability boundary, though the estimated B_{10} lifetime appears longer. In other words, the reliability of the system is constrained by the stability.

Therefore, to further improve the reliability performance of the entire system, it is practical to modify the controllers to enhance the system stability. In this article, two approaches will be introduced in this aspect: modifying the low-pass filter (LPF) of power in the droop control, or using a power system stabilizer (PSS) consisting of a lead-lag compensator.

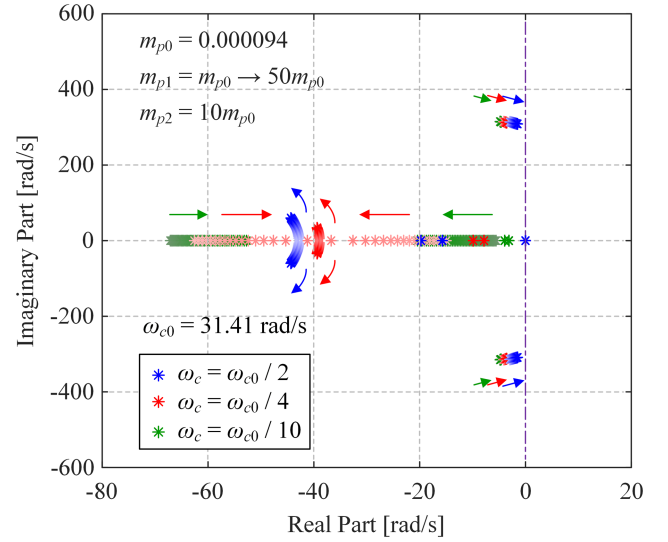


Fig. 7. Eigenvalue loci of the example system when the active droop gain of converter 1 ranges from m_{p0} to $50 m_{p0}$.

C. Stability Enhancement by Low-Pass Filter

An LPF in the droop control is employed to obtain the dc component of the active and reactive power. As presented in Section III-A, the frequency undergoes divergent oscillations when instability occurs. Therefore, decreasing its bandwidth may help to enhance the system stability to some extent by suppressing the frequency oscillation.

In the study case, the eigenvalue loci when the bandwidth of the LPF varies are plotted in Fig. 7. The cutoff frequency of the LPF is modified into 5%, 2.5%, and 1% of the fundamental frequency. When the bandwidth of the LPF decreases, the dominant pair of poles move further away from the RHP. Though the poles are still approaching the imaginary axis for large droop gains, the stability margin of the system could become larger.

Simulations have been conducted to illustrate the feasibility of this approach. The cutoff frequency ω_c is decreased to $\omega_{c0}/2$, or 5% of the fundamental angular frequency ω_1 . The system remains stable until m_{p1} is increased to $50 m_{p0}$. In comparison with Fig. 4, there could be more options for the droop gains, leading to more possibilities for a longer lifetime of the system.

It should also be noted that a lower bandwidth ω_c also indicates more control delays, or larger inertia (slower dynamics) of the converter. If ω_c is further decreased, the dynamic performance of the system will be largely influenced, resulting in longer settling time t_s and larger overshoot during settling in Fig. 8 when there is a transient in the system. This issue could further aggravate, when the voltage is controlled by double closed-loop controllers [28] in practice.

D. Stability Enhancement by Power System Stabilizer

To mitigate the oscillations in frequency, it is also practical to compensate the frequency by a PSS using a lead-lag compensator [30], which is shown in Fig. 9. The tuning procedure of this PSS is relatively easy to follow compared to other stabilizers like [31], [32], and such PSS based on harmonic compensation

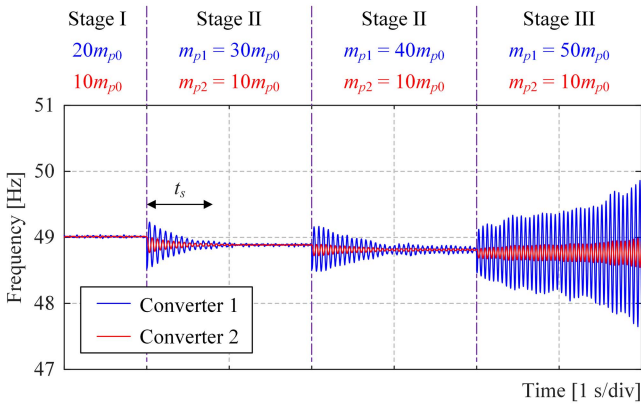


Fig. 8. Frequencies of the two converters when the droop gain of converter 1 is increased. The cutoff frequency ω_c is decreased to $\omega_{c0}/2$.

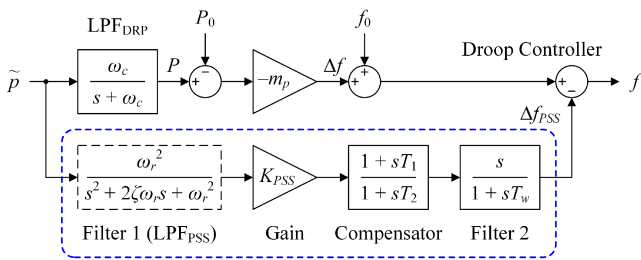


Fig. 9. Modified active power control with a PSS.

does not influence the power sharing among converters. In principle, a signal with the same amplitude and opposite phase of the frequency oscillation is generated, such that the particular oscillation can be compensated to zero.

The PSS is designed based on the procedure in [30], including the following.

- 1) *Lead-Lag Compensator (Compensator in Fig. 9)*: At the oscillation frequency, the phase response of the compensator should be complimentary to that of the LPF in the droop controller (LPF_{DRP}).
- 2) *Washout Filter (filter 2 in Fig. 9)*: The washout filter is used to suppress the dc offset in the measured active power \tilde{p} . Its phase response at the oscillation frequency should be sufficiently small, such that it causes negligible influence to the phase of the oscillation component.
- 3) *Gain of the PSS K_{PSS}* : It is critical in the compensation that the gain through the path of the droop controller is the same as that of the PSS. K_{PSS} is designed to ensure this.

Furthermore, to minimize the influence of high-order harmonics (e.g., switching-frequency harmonics) in the measured power and smoothen the compensation signal, another LPF can be alternatively added in the PSS, which is filter 1 in Fig. 9 and denoted as LPF_{PSS}. Compared to the LPF_{DRP}, the LPF_{PSS} should not affect the phase of the oscillation component significantly, but should be able to suppress high-order harmonics as well. A second-order LPF is thereby used in this article. Its cut-off frequency is designed to be between the oscillation frequency and the frequency of harmonics to be suppressed, while the damping ratio is a tradeoff between the suppression

TABLE II
DESIGNED PARAMETERS OF THE PSS IN THE STUDY CASE

Variables of the PSS	Values	Units
Time constant T_1	0.04178	s
Time constant T_2	0.0001	s
Time constant T_w	3	s
Gain of the PSS for Converter 2 K_{PSS2}	0.0000286	—
Resonance frequency of the LPF _{PSS} ω_r	1570	rad/s
Damping ratio of the LPF _{PSS} ζ	0.025	—

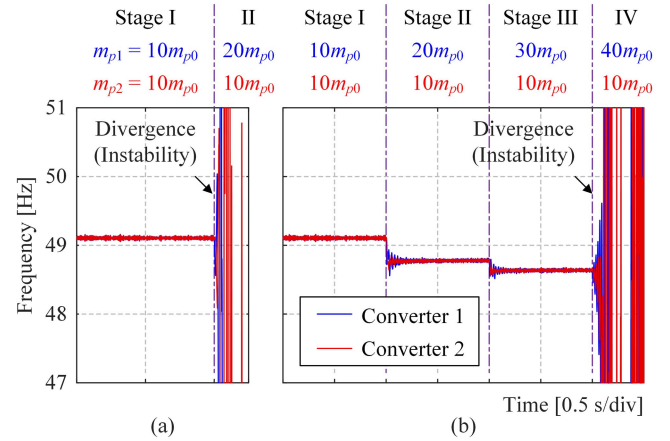


Fig. 10. Frequencies of the two converters when the droop gain of Converter 1 is increased and voltage loops are considered. (a) Without PSS. (b) With PSS employed in both converters.

of overshoots during transients and the minimization of phase shifts at the oscillation frequency.

In the studied case, the oscillation of frequency is measured as 271 rad/s, and the phase delay at this frequency caused by the LPF_{DRP} is -83.4° . Based on the design procedure in [30], a group of PSS parameters can be designed as shown in Table II. It should be noted that the gain of the PSS K_{PSS} in Table II is the gain for converter 2 K_{PSS2} , while the gain for converter 1 K_{PSS1} is calculated proportionally based on the two droop gains, i.e., $K_{PSS1} = K_{PSS2} \times m_{p1}/m_{p2}$.

Simulations have also been conducted to validate the performance of the PSS, wherein the voltage loops are considered. The frequencies of the two converters are shown in Fig. 10, and the cases without the PSS and with the PSS are compared when m_{p1} increases. The results show that, by employing the PSS in Fig. 10(b), the system will be much more stable than Fig. 10(a). The compensation of the frequency oscillation could also extend the boundary of system reliability under stability constraints, as it allows further increase of the droop gains.

IV. FRAMEWORK OF STABILITY-CONSTRAINED RELIABILITY-ORIENTED DROOP CONTROL IN MICROGRIDS

To address the aforementioned issues in a more coherent way, it is critical to integrate stability analysis on the systems into the reliability-oriented control or design. The framework of stability-constrained reliability-oriented droop control for microgrids is thereby proposed as shown in Fig. 11.

The entire framework includes both the reliability and stability techniques. In reliability-oriented droop control, the power flow

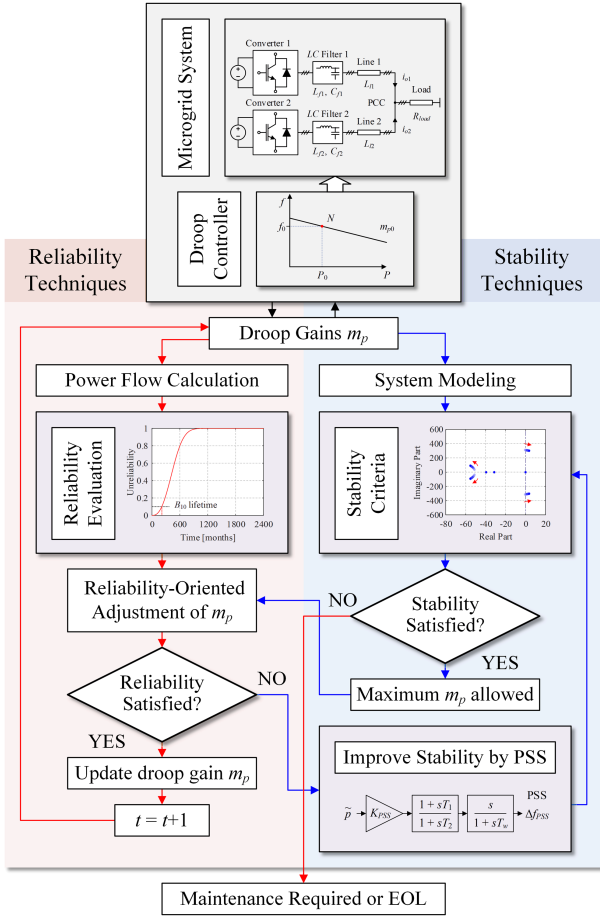


Fig. 11. Framework of stability-constrained reliability-oriented droop control for microgrids.

is calculated to obtain the system reliability, and the droop gain is adjusted based on the performances of converters and updated every certain period, whereas stability criteria now act additionally as the constraints of the droop adjustment. The stability criteria can be either the aforementioned small-signal stability or voltage or frequency constraints in terms of the droop relationship. If stability cannot be satisfied, the reliability performance should be reconsidered; or stability should be improved by, e.g., by using a PSS. If both stability and reliability performances cannot be satisfied in the system, then maintenance might be required. This could happen when, e.g., the system is approaching its EOL.

Remark 1: In this framework, both power flow calculation and stability modeling involve system-level coordination, yet there is not necessarily a strong requirement of communication among converters as the droop gains can be updated by secondary or tertiary control period, e.g., by month.

Remark 2: This framework addresses the stability concern in the reliability-oriented power sharing specified in (10) and (11). For other reliability-oriented control strategies, system stability should be likewise speculated to ensure safe operation.

V. EXPERIMENTAL TESTS AND LONG-TERM VALIDATIONS

To better illustrate the issue addressed in this article and validate the proposed framework, experiments and long-term reliability evaluations are presented in this section.

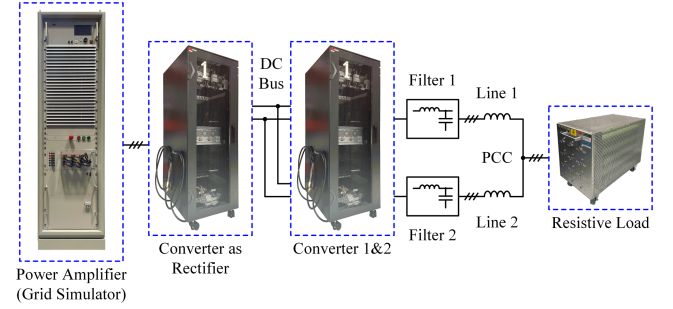


Fig. 12. Experimental setup, where two three-phase DC–AC converters are installed in each converter rack.

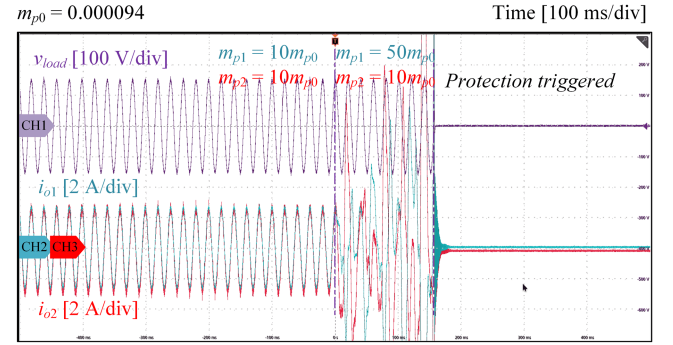


Fig. 13. Load voltage and output currents of the two converters when the droop gain of converter 1 is increased from $10 m_{p0}$ to $50 m_{p0}$.

A. Experimental Tests of Instability

The experimental setup is shown in Fig. 12, in which the topology is similar to that in Fig. 3. Two 7-kW dc–ac converters operate as the converters 1 and 2 respectively, and inductors are employed as the line impedances. The load resistance is downscaled to 28.75Ω due to the available hardware resources, but the other parameters remain the same as given in Table I unless specified otherwise.

The instability when the droop gain increases from $10 m_{p0}$ to $50 m_{p0}$ is illustrated in Fig. 13, where the voltage at PCC (load voltage) and the two output currents i_{o1} and i_{o2} are measured. The protection inside the setup is triggered due to the subsequent overcurrent after the transient, which indicates that there is a boundary of stability for the power sharing.

The instability is also illustrated under smaller transients, where the droop gain of converter 1 m_{p1} is increased from $16 m_{p0}$ to $20 m_{p0}$. It is shown in Fig. 14(a) that the instability appears in the form of frequency oscillation, and in Fig. 14(b), the oscillation is reflected in the current as low-frequency oscillation.

The experimental results agree with the discussions and simulations in Section III-A, showing that the instability could arise if one or more droop gains are increased for the sake of reliability enhancement. The stability criteria are limiting the boundary of the system performance.

B. Experimental Tests of Stability Enhancement by PSS

Moreover, based on the setup in Section V-A, a PSS is employed in the experiments to enhance the system stability. In this case, it is measured that the oscillation of frequency is

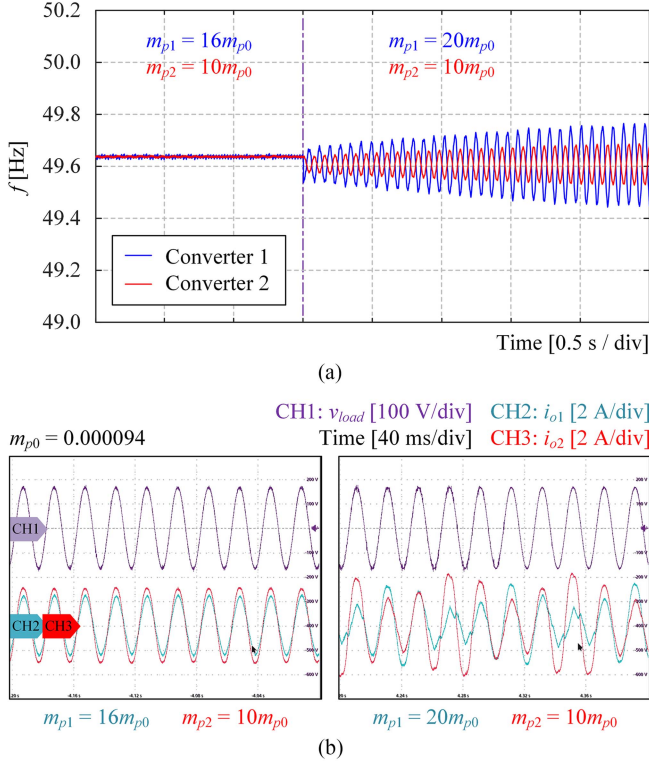


Fig. 14. Instability when the droop gain of Converter 1 is increased from $16 m_{p0}$ to $20 m_{p0}$, including: (a) the divergent frequency of the two converters and (b) the load voltage v_{load} and the two output currents i_{o1} and i_{o2} .

TABLE III

DESIGNED PARAMETERS OF THE PSS IN THE EXPERIMENTS

Variables of the PSS	Values	Units
Time constant T_1	0.0421	s
Time constant T_2	0.001	s
Time constant T_w	3	s
Gain of the PSS for Converter 2 K_{PSS2}	0.000275	—
Resonance frequency of the LPF _{PSS} ω_r	942	rad/s
Damping ratio of the LPF _{PSS} ζ	0.02	—

83.14 rad/s, and the phase delay is -69.3° . Similar to Section II-D, the PSS parameters can be designed as given in Table III.

The experimental results are shown in Fig. 15. With the PSS, the oscillation when $m_{p1} = 20 m_{p0}$ is well compensated, and the system could reach a new steady state. Besides, when the droop gain m_{p1} is further increased to $20 m_{p0}$, the system can still operate without divergence in stability. Hence, it can be concluded that the PSS has much potential to enhance the system stability.

However, it should also be noted in Fig. 15 that the frequency is decreasing due to the droop relationship given in (9), when the droop gain m_{p1} increases. This means that in practice, the limit of frequency is also a critical concern, so that the power capacities of the sources and lines are not violated.

C. Long-Term Evaluation of Reliability

Moreover, a power system based on the CIGRE low-voltage benchmark network in [33] is selected as a study case, to illustrate the significance of stability constraints in long-term

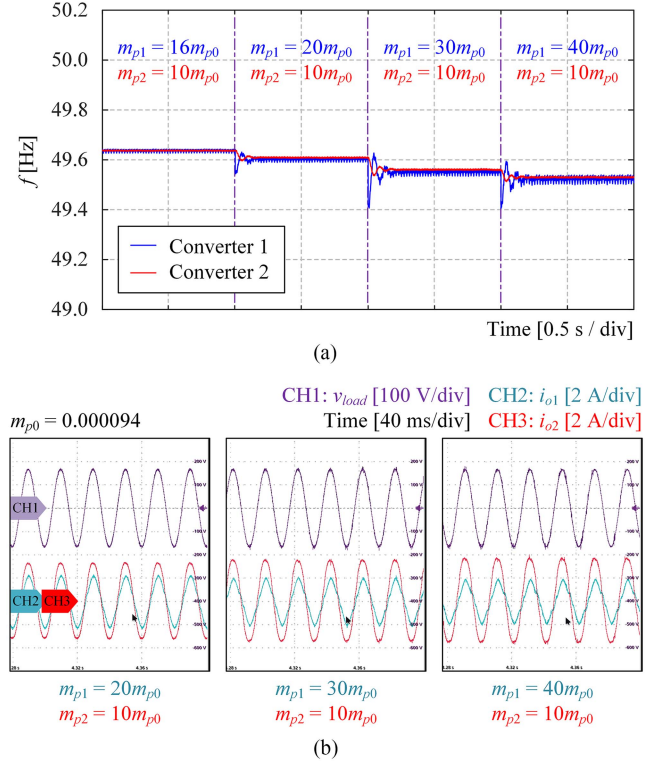


Fig. 15. Effects of the PSS when the droop gain of Converter 1 is increased from $16 m_{p0}$ to $40 m_{p0}$, including: (a) the frequency of the two converters and (b) the load voltage v_{load} and the two output currents i_{o1} and i_{o2} .

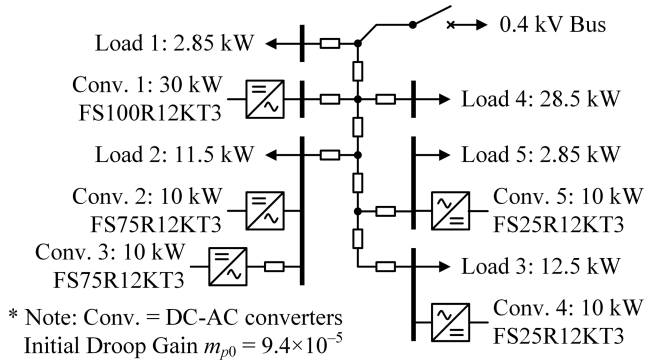


Fig. 16. Structure of the power system for long-term reliability evaluation.

reliability performance. The system is shown in Fig. 16, which is an ac microgrid consisting of five dc-ac converters and five resistive loads, and the system operates in islanded mode. Key parameters related to reliability evaluations are given in Table IV. It is also assumed here that the degradation of capacitors is not considered, and the types of the power devices are selected differently for the converters, so that the power sharing could make more difference in the system reliability.

The reliability performance of the system is evaluated when the droop gains of converters 2 and 3 m_{p2} and m_{p3} are changed, as shown in Fig. 17. Compared with the example in Fig. 6, the system consists of more converters and thus has much shorter estimated lifetime. When different power sharing among

TABLE IV
KEY PARAMETERS OF THE STUDY CASE ON LONG-TERM PERFORMANCE

Parameters	Values
Nominal AC voltage V_n	230 V _{RMS} , 50 Hz
Types of the power devices	FS100R12KT3 for Converter 1 FS75R12KT3 for Converters 2 and 3 FS25R12KT3 for Converters 4 and 5
Initial active droop gain m_{p0}	9.4×10^{-5} [Hz/W]
Power cycling period t_{on}	0.01 s
Number of cycles per month	$(24 \times 60 \times 60 \times 30) \times 50$

Note: V_{RMS} = Volts in Root-Mean-Square (RMS) value.

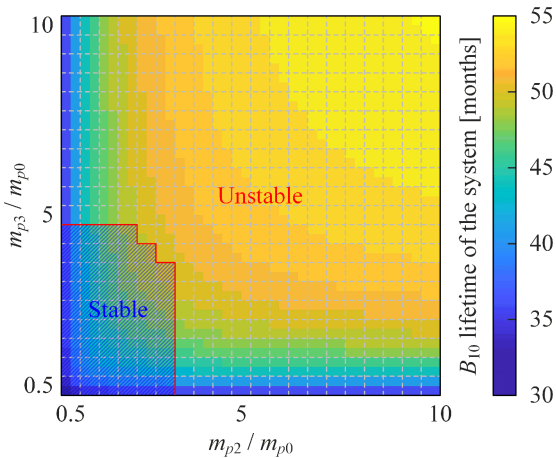


Fig. 17. Estimated lifetime of the system in terms of the variation of droop gains m_{p2} and m_{p3} . The stable region of the system is also marked as the shaded area.

converters is achieved under different droop gains, the estimated lifetime of the system could vary from around 30 months to 55 months, but the stability of the system is limiting the lifetime to around 45–50 months. It is shown that stability analysis is of significance in reliability evaluations, and that enlarging the stability region could contribute to a higher reliability of the entire system.

VI. CONCLUSION

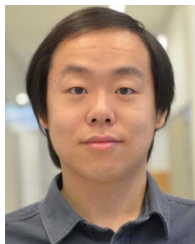
In this article, the instability in reliability-oriented droop control has been revealed and analyzed. Instability may occur due to the adjustment of droop gains, and accordingly, solutions have been applied to enhance the stability of the system and to further prolong the lifetime of the system via reliability-oriented power sharing. The feasibility of the techniques has been validated by simulations and experiments.

Besides, a relationship between the stability and reliability of microgrid systems has also been revealed from the analysis: the stability is bounding the reliability, and should be taken into consideration in reliability design and control. The evaluation of system performance combining stability and reliability can potentially be a more practical guideline for the design and operation of microgrids. To extend the scope of this article in the future, the stability constraints can also be generalized as a time-variant performance, which can be regularly updated based on, e.g., mission profiles, power grid profiles, or maintenances.

REFERENCES

- [1] D. Boroyevich, I. Cvetković, D. Dong, R. Burgos, F. F. Wang, and F. C. Lee, "Future electronic power distribution systems - a contemplative view," in *Proc. 12th Int. Conf. Optim. Elect. Electron. Equip.*, 2010, pp. 1369–1380.
- [2] J. M. Carrasco et al., "Power-electronic systems for the grid integration of renewable energy sources: A survey," *IEEE Trans. Ind. Electron.*, vol. 53, no. 4, pp. 1002–1016, Jun. 2006.
- [3] H. Wang et al., "Transitioning to physics-of-failure as a reliability driver in power electronics," *IEEE J. Emerg. Sel. Topics Power Electron.*, vol. 2, no. 1, pp. 97–114, Mar. 2014.
- [4] J. Falck, C. Felgemacher, A. Rojko, M. Liserre, and P. Zacharias, "Reliability of power electronics systems: An industry perspective," *IEEE Ind. Electron. Mag.*, vol. 12, no. 2, pp. 24–35, Jun. 2018.
- [5] S. Peyghami, P. Palensky, and F. Blaabjerg, "An overview on the reliability of modern power electronic based power systems," *IEEE Open J. Power Electron.*, vol. 1, pp. 34–50, 2020.
- [6] M. H. Ling, K. L. Tsui, and N. Balakrishnan, "Accelerated degradation analysis for the quality of a system based on the gamma process," *IEEE Trans. Rel.*, vol. 64, no. 1, pp. 463–472, Mar. 2015.
- [7] S. Guo et al., "Operational lifetime-stress model for complex networks," *IEEE Trans. Rel.*, vol. 71, no. 3, pp. 1255–1263, Sep. 2022.
- [8] R. Burgos, G. Chen, F. F. Wang, D. Boroyevich, W. G. Odendaal, and J. D. van Wyk, "Reliability-oriented design of three-phase power converters for aircraft applications," *IEEE Trans. Aerosp. Electron. Syst.*, vol. 48, no. 2, pp. 1249–1263, Apr. 2012.
- [9] D. Zhou, H. Wang, and F. Blaabjerg, "Mission profile based system-level reliability analysis of DC/DC converters for a backup power application," *IEEE Trans. Power Electron.*, vol. 33, no. 9, pp. 8030–8039, Sep. 2018.
- [10] Q. Xu, Y. Xu, P. Tu, T. Zhao, and P. Wang, "Systematic reliability modeling and evaluation for on-board power systems of more electric aircrafts," *IEEE Trans. Power Syst.*, vol. 34, no. 4, pp. 3264–3273, Jul. 2019.
- [11] M. Andresen, K. Ma, G. Buticchi, J. Falck, F. Blaabjerg, and M. Liserre, "Junction temperature control for more reliable power electronics," *IEEE Trans. Power Electron.*, vol. 33, no. 1, pp. 765–776, Jan. 2018.
- [12] M. Andresen, V. Raveendran, G. Buticchi, and M. Liserre, "Lifetime-based power routing in parallel converters for smart transformer application," *IEEE Trans. Ind. Electron.*, vol. 65, no. 2, pp. 1675–1684, Feb. 2018.
- [13] J. Jiang, S. Peyghami, C. Coates, and F. Blaabjerg, "A decentralized reliability-enhanced power sharing strategy for PV-based microgrids," *IEEE Trans. Power Electron.*, vol. 36, no. 6, pp. 7281–7293, Jun. 2021.
- [14] I. U. Nutkani, P. C. Loh, P. Wang, and F. Blaabjerg, "Cost-prioritized droop schemes for autonomous AC microgrids," *IEEE Trans. Power Electron.*, vol. 30, no. 2, pp. 1109–1119, Feb. 2015.
- [15] M. Farrokhabadi et al., "Microgrid stability definitions, analysis, and examples," *IEEE Trans. Power Syst.*, vol. 35, no. 1, pp. 13–29, Jan. 2020.
- [16] N. Pogaku, M. Prodanovic, and T. C. Green, "Modeling, analysis and testing of autonomous operation of an inverter-based microgrid," *IEEE Trans. Power Electron.*, vol. 22, no. 2, pp. 613–625, Mar. 2007.
- [17] J. Sun, "Impedance-based stability criterion for grid-connected inverters," *IEEE Trans. Power Electron.*, vol. 26, no. 11, pp. 3075–3078, Nov. 2011.
- [18] X. Wang, F. Blaabjerg, and W. Wu, "Modeling and analysis of harmonic stability in an AC power-electronics-based power system," *IEEE Trans. Power Electron.*, vol. 29, no. 12, pp. 6421–6432, Dec. 2014.
- [19] Y. Song, S. Sahoo, Y. Yang, and F. Blaabjerg, "Quantitative mapping of modeling methods for stability validation in microgrids," *IEEE Open J. Power Electron.*, vol. 3, pp. 679–688, 2022.
- [20] Y. Song, S. Sahoo, Y. Yang, and F. Blaabjerg, "System-level stability of the CIGRE low voltage benchmark system: Definitions and extrapolations," in *Proc. IEEE 22nd Workshop Control Model. Power Electron.*, 2021, pp. 1–6.
- [21] H. Farzin, M. Fotuhi-Firuzabad, and M. Moeini-Aghtaie, "Role of outage management strategy in reliability performance of multi-microgrid distribution systems," *IEEE Trans. Power Syst.*, vol. 33, no. 3, pp. 2359–2369, May 2018.
- [22] S. Yang, A. Bryant, P. Mawby, D. Xiang, L. Ran, and P. Tavner, "An industry-based survey of reliability in power electronic converters," *IEEE Trans. Ind. Appl.*, vol. 47, no. 3, pp. 1441–1451, May/Jun. 2011.
- [23] R. Bayerer, T. Herrmann, T. Licht, J. Lutz, and M. Feller, "Model for power cycling lifetime of IGBT modules - various factors influencing lifetime," in *Proc. 5th Int. Conf. Integr. Power Electron. Syst.*, 2008, pp. 1–6.
- [24] "AN2019-05: PC and TC diagrams, Rev. 2.1," Infineon, Feb. 2021. [Online]. Available: https://www.infineon.com/dgdl/Infineon-AN2019-05_PC_and_TC_Diagrams-ApplicationNotes-v02_01-EN.pdf?fileId=5546d46269e1c019016a594443e4396b, Accessed: Apr. 2022.

- [25] M. A. Miner, "Cumulative damage in fatigue," *J. Appl. Mech.*, vol. 12, no. 3, pp. A159–A164, 1945.
- [26] H. Wang and F. Blaabjerg, "Reliability of capacitors for DC-link applications in power electronic converters - an overview," *IEEE Trans. Ind. Appl.*, vol. 50, no. 5, pp. 3569–3578, Sep./Oct. 2014.
- [27] S. Peyghami, P. Davari, and F. Blaabjerg, "System-level reliability-oriented power sharing strategy for DC power systems," *IEEE Trans. Ind. Appl.*, vol. 55, no. 5, pp. 4865–4875, Sep./Oct. 2019.
- [28] J. Rocabert, A. Luna, F. Blaabjerg, and P. Rodríguez, "Control of power converters in AC microgrids," *IEEE Trans. Power Electron.*, vol. 27, no. 11, pp. 4734–4749, Nov. 2012.
- [29] Y. Song, S. Sahoo, Y. Yang, and F. Blaabjerg, "Conditional droop adjustment for reliability-oriented power sharing in microgrids," *IEEE Trans. Circuits Syst. II Exp. Briefs*, to be published, doi: [10.1109/TC-SII.2023.3242139](https://doi.org/10.1109/TC-SII.2023.3242139).
- [30] A. Firdaus and S. Mishra, "Mitigation of power and frequency instability to improve load sharing among distributed inverters in microgrid systems," *IEEE Syst. J.*, vol. 14, no. 1, pp. 1024–1033, Mar. 2020.
- [31] R. Majumder, B. Chaudhuri, A. Ghosh, R. Majumder, G. Ledwich, and F. Zare, "Improvement of stability and load sharing in an autonomous microgrid using supplementary droop control loop," *IEEE Trans. Power Syst.*, vol. 25, no. 2, pp. 796–808, May 2010.
- [32] M. B. DeJhavi and A. Yazdani, "An adaptive feedforward compensation for stability enhancement in droop-controlled inverter-based microgrids," *IEEE Trans. Power Del.*, vol. 26, no. 3, pp. 1764–1773, Jul. 2011.
- [33] S. Papathanassiou, N. D. Hatziargyriou, and K. Strunz, "A benchmark low voltage microgrid network," in *Proc. CIGRE Symp., Power Syst. Dispersed Gener.*, 2005, pp. 1–8.



Yubo Song (Student Member, IEEE) received the B.Sc. and M.Eng. degrees in electrical engineering from Shanghai Jiao Tong University, Shanghai, China, in 2016 and 2019, respectively. He is currently working toward the Ph.D. degree with the Department of Energy, Aalborg University (AAU Energy), Aalborg, Denmark, on the stability and reliability of microgrids.

From May to July 2022, he was a Visiting Researcher with the University of Alberta, Edmonton, AB, Canada. His research interests include the control, stability and reliability of power electronic systems.



Subham Sahoo (Senior Member, IEEE) received the B.Tech. degree in electrical and electronics engineering from Veer Surendra Sai University of Technology, Burla, India, in 2014, and the Ph.D. degree in electrical engineering from the Indian Institute of Technology, Delhi, New Delhi, India, in 2018, respectively.

He is currently an Assistant Professor with the Department of Energy, Aalborg University, Denmark, where he is also the Vice-Leader of the research group on Reliability of Power Electronic Converters (ReliaPEC) in AAU Energy. He is selected into EU-US

National Academy of Engineering Frontier of Engineering Class of 2021. His research interests are control, optimization, cybersecurity and stability of power electronic dominated grids, application of artificial intelligence and machine learning in power electronic systems.

Dr. Sahoo was also a Distinguished reviewer for IEEE TRANSACTIONS ON SMART GRID in 2020. He is currently the Vice-chair of IEEE PELS Technical Committee 10 on Design Methodologies. He is an Associate Editor for IEEE TRANSACTIONS ON TRANSPORTATION ELECTRIFICATION. He is a recipient of the Indian National Academy of Engineering Innovative Students Project Award for the best Ph.D. thesis across all the institutes in India for the year 2019.



Yongheng Yang (Senior Member, IEEE) received the B.Eng. degree in electrical engineering and Automation from Northwestern Polytechnical University, Xi'an, China, in 2009, the Postgraduate degree from Southeast University, Nanjing, China, in 2011, and the Ph.D. degree in energy technology from Aalborg University, Aalborg, Denmark, in 2014.

He was a Visiting Scholar with Texas A&M University, College Station, TX, USA, during March–May 2013. From 2014 to 2020, he was with the Department of Energy Technology, Aalborg University, where he achieved the rank of tenured an Associate Professor in 2018. In January 2021, he was a Professor with Zhejiang University, China. He was a Zhejiang Kunpeng Investigator in 2023. His research interests include on grid-integration of photovoltaic systems and control of power converters, specifically grid-forming control technologies.

Dr. Yang was the Chair of the IEEE Denmark Section in 2019–2020 and is an Associate Editor for several IEEE TRANSACTIONS. He was the recipient of the 2018 IET Renewable Power Generation Premium Award and was recognized as an Outstanding Reviewer for the IEEE TRANSACTIONS ON POWER ELECTRONICS in 2018. He was the recipient of the 2021 Richard M. Bass Outstanding Young Power Electronics Engineer Award from the IEEE Power Electronics Society and the 2022 IEEE Isao Takahashi Power Electronics Award. In addition, he has received two IEEE Best Paper Awards. He was included on the list of the Highly Cited Chinese Researchers by Elsevier in 2022–2023. He is currently the Vice Chair of the IEEE PELS Technical Committee on Sustainable Energy Systems and a Council Member of the China Power Supply Society.



Frede Blaabjerg (Fellow, IEEE) received the Ph.D. degree in electrical engineering from Aalborg University, Aalborg, Denmark, in 1995 and the Honoris Causa degree from University Politehnica Timisoara, Timisoara, Romania, in 2017, and Tallinn Technical University, Tallinn, Estonia, in 2018.

He was with ABB-Scandia, Randers, Denmark, from 1987 to 1988. He was an Assistant Professor in 1992, an Associate Professor in 1996, and a Full Professor of power electronics and drives in 1998. In 2017, he was a Villum Investigator. He has authored

or coauthored more than 600 journal papers in the fields of power electronics and its applications. He is the co-author of four monographs and editor of ten books in power electronics and its applications. His current research interests include power electronics and its applications, such as in wind turbines, PV systems, reliability, harmonics, and adjustable speed drives

Dr. Blaabjerg he was the recipient of 32 IEEE Prize Paper Awards, the IEEE PELS Distinguished Service Award in 2009, the EPE-PEMC Council Award in 2010, the IEEE William E. Newell Power Electronics Award 2014, the Villum Kann Rasmussen Research Award 2014, the Global Energy uPrize in 2019 and the 2020 IEEE Edison Medal. He was the Editor-in-Chief for IEEE TRANSACTIONS ON POWER ELECTRONICS, from 2006 to 2012. He has been a Distinguished Lecturer for the IEEE Power Electronics Society from 2005 to 2007 and for the IEEE Industry Applications Society from 2010 to 2011 as well as 2017 to 2018. During 2019–2020, he was the President of the IEEE Power Electronics Society. He is the Vice-President of the Danish Academy of Technical Sciences too. He is nominated in 2014–2019 by Thomson Reuters to be between the most 250 cited researchers in engineering in the world.